Far-infrared rotational spectrum of HD: Line shape, dipole moment, and collisional interference

P. G. Drakopoulos and G. C. Tabisz

Department of Physics, University of Manitoba, Winnipeg, Manitoba, Canada R3T 2N2

The rotational transitions $R(0)$ to $R(3)$ in pure HD gas have been studied in absorption with 0.06-cm^{-1} resolution at densities from 2 to 68 amagat at 295 K. The permanent dipole moment of HD was found to be 8.83(28), 7.94(2), 7.88(3), and 8.43(10) for $R(0)$ to $R(3)$, respectively, in units of 10^{-4} D. These are in general agreement with *ab initio* calculations except for an unpredicted strong rotational state dependence. Collisional interference was observed and the interference parameter, proportional to the ratio of the average induced dipole moment to the allowed moment, is negative for $R(0)$ and $R(1)$, positive for $R(2)$ and $R(3)$, and of a magnitude consistent with calculation. Comparisons are made with earlier work, particularly that of McKellar [Can. J. Phys. **64**, 227 (1986)].

I. INTRODUCTION

The far-infrared rotational absorption spectrum of HD has recently been the subject of several studies and the source of some debate. Following the discovery[1,2] of an anomalous behavior of intensity as a function of density in the vibration rotation spectrum of HD, a theoretical interpretation[2−5] was advanced in terms of an interference between allowed and collision-induced transitions. Immediately the suggestion was made[3] that lack of knowledge of this effect had flawed an earlier analysis[6] of the far-infrared spectrum and determination of the permanent dipole moment. Several experimental studies[7−11] followed reporting the magnitude of the dipole moment and the nature of the interference phenomenon. These found values of the dipole moment generally within better than 15% of *ab initio* calculations. There remained, however, disagreement about the precise value of the moment, its dependence on rotational quantum number, and the magnitude and sign of the interference. The present study was undertaken in an attempt to clarify these issues.

In order to take a systematic approach to characterization of the interference, a series of experiments was performed that included, in addition to pure HD, mixtures with all inert gases, H_2 and N_2; total pressures ranged between 2 and 100 atm at 295 K. This paper presents the necessary theoretical background and discusses the spectrum of pure HD. In particular, in Sec. II, the theoretical foundations are reviewed. The experimental procedure is described in Sec. III. In Sec. IV, the data are presented and the dipole moment, interference parameter, and spectral line parameters are compared with earlier studies. Finally, in Sec. V, a calculation of the magnitude of the interference is performed with the existing theory. The spectra of the mixtures is the subject of paper II in this series.[12]

II. THEORETICAL CONCEPTS

Collision-induced spectra occur quite generally and are due to absorption by the transient dipole created in a pair or larger cluster of interacting molecules.[13] If one or more of these molecules also has a permanent moment, then interference between allowed and induced transition moments may take place. Depending on the relative signs of the moments, the interference can be either constructive or destructive and enhancement or reduction of the absorption coefficient, respectively, will occur. The fact that the allowed moment in HD is so small makes it a unique case for studying collisionally induced phenomena in allowed spectra.[2] Normally such effects are overshadowed by the strong allowed absorption.

The absorption coefficient at frequency ω is given by

$$\alpha(\omega) = (1/L)\ln[I_0(\omega)/I(\omega)]$$
$$= \rho N_0 (4\pi^2/3\hbar c)\omega[1 - \exp(\hbar\omega/kT)]\phi(\omega) . \quad (1)$$

Here L is the optical path length, I_0 and I are the intensities transmitted in the absence and presence of the absorber, ρ is the density in amagat, N_0 is Loschmidt's number, and $\phi(\omega)$ is the spectral density function,

$$\phi(\omega) = (1/\pi)\text{Re} \int_0^\infty \exp(-i\omega t)C(t)dt , \quad (2)$$

with

$$C(t) = \langle \mu(0)\cdot\mu(t) \rangle . \quad (3)$$

The dipole moment operator $\mu(t)$ represents all possible moments in the spectrum, both allowed and induced. In the following discussion, emphasis is given to mechanisms important to the intensity and shape of the sharp features appearing in the spectrum at the positions of the pure rotational transitions which follow the selection rule $\Delta J = +1$; J is the rotational quantum number.

A. The permanent dipole moment of HD

The hydrogen isotope HD possesses a small allowed electric dipole moment due to nonadiabatic effects coupling electronic and nuclear motions. Wick[14] predicted its existence and many authors have attempted its calculation by *ab initio* methods. The most recent and most

elaborate calculations are by Wolniewicz,[15] Ford and Browne,[16] and Thorson et al.[17] Interestingly, in this last reference, a coordinate transformation is employed such that the isotopically induced asymmetry appears directly in the electronic Hamiltonian and the moment is derived within the clamped nuclei approximation. The matrix elements of the moment can be written[15] as vibrational-rotational matrix elements of $p^A(r)$, a function of only internuclear separation r. The value of $p^A(r)$ at r_e, the equilibrium internuclear separation, is termed the permanent dipole moment and is given by computation as $\sim 8.4 \times 10^{-4}$ D. It lies along the internuclear axis in the direction H^+D^-; that is, it points from H to D and is

negative in a coordinate system whose z axis points from D to H (Fig. 1).

B. The collision-induced moment

The symmetric molecule H_2 does not have an allowed dipole moment and does not exhibit an allowed infrared spectrum. It does, however, have a collision-induced spectrum which has been fully studied.[13] The mechanisms which generate the induced dipole are closely related to the interaction terms in the molecular potential, namely induction, dispersion, and exchange.

For two interacting molecules, the ν component of the pair dipole moment μ^I may be expressed as[18]

$$\mu_\nu^I(r_1 r_2; R) = \frac{(4\pi)^{3/2}}{\sqrt{3}} \sum_{\lambda_1, \lambda_2, \Lambda, \lambda} A_\Lambda(\lambda_1, \lambda_2, \lambda; r_1, r_2, R)$$

$$\times \sum_{\mu, \mu_2} C(\lambda_1, \lambda_2, \Lambda; \nu-\mu-\mu_2, \mu_2) C(\Lambda, \lambda, 1; \nu-\mu, \mu) Y_{\lambda_1, \nu-\mu-\mu_2}(\omega_1) Y_{\lambda_2, \mu_2}(\omega_2) Y_{\lambda, \mu}(\Omega) . \quad (4)$$

The angles ω_1, ω_2, and Ω describe the orientation of molecules 1 and 2 and of the intermolecular axis relative to a laboratory fixed reference frame; r_1 and r_2 are the internuclear separations; R is the intermolecular distance (Fig. 1). The symbols C and Y denote Clebsch-Gordon coefficients and spherical harmonics. The coefficients A_Λ provide a coordinate-independent classification of the various components of the induced moment.

A number of these coefficients have been evaluated quantitatively: anisotropic quadrupolar induction $A_2(223)$, isotropic overlap $A_0(001)$, anisotropic overlap $A_2(201)$; $A_1(100)$ describes a dipole along the internu-
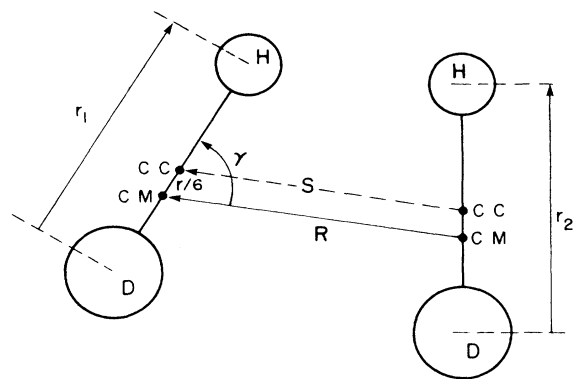

FIG. 1. Coordinate system for two HD molecules. CM is the center of mass; CC is the center of charge. The internuclear separation in molecules 1 and 2 is denoted by r_1 and r_2; R is the distance between the centers of mass and S is the distance between the midpoints of the molecules. The angle γ is between an internuclear axis and the intermolecular axis. Angles ω_1, ω_2, and Ω (not shown) are used in Eq. (4) to describe the orientations of the internuclear axes of molecules 1 and 2 and of the intermolecular vector R relative to a laboratory fixed reference frame. For the case of an HD-atom interaction, r_2 is set to zero.

clear axis of 1, which vanishes for H_2-H_2 but does not for systems involving HD.

The pair HD-HD, within the adiabatic approximation, is similar to H_2-H_2. The same induced dipole moment applies to both situations provided a requisite coordinate transformation is made. Induced moments are analyzed with respect to the molecular centers of mass. For HD, the centers of mass and of charge are displaced by a small distance $r/6$ (Fig. 1). If S is the distance between the midpoints of the two molecules, then

$$\mathbf{S} = \mathbf{R} + (1/6)(\mathbf{r}_1 - \mathbf{r}_2)$$

and, to a first approximation,

$$\mu^I(\text{HD-HD}) = [1 + (\tfrac{1}{6})(\mathbf{r}_1 - \mathbf{r}_2) \cdot \nabla_R] \mu^I(H_2 - H_2) . \quad (5)$$

New odd components of A_Λ are thereby generated from (4) which permit the transitions $\Delta J = \pm 1, \pm 3, \ldots$, in addition to the $\Delta J = 0, \pm 2, \ldots$, transitions which are allowed and observed in H_2-H_2. These new symmetries are responsible for spectral features unique to the HD-HD system.[2,3,19,20]

C. Collisional interference

The total dipole moment in a system of N molecules is then

$$\mu(t) = \mu^A(t) + N\mu^I(t) .$$

When $\mu(t)$ is substituted into (2), the spectrum is seen to consist of several parts.

1. Allowed

The allowed spectrum arises from terms $\langle \mu_1^A(0) \cdot \mu_1^A(t) \rangle$. In the impact approximation the line shape is a pressure-broadened Lorentzian contour. The contribution to the absorption coefficient (1) depends linearly on the density ρ.

2. Allowed-induced

The cross terms $\langle \mu_1^A(0)\cdot\mu_{12}^I(t)\rangle$ and $\langle \mu_{12}^I(0)\cdot\mu_1^A(t)\rangle$ represent interference between allowed and induced moments.[5] The mechanism involves two molecules and depends upon the density squared. If interference is to occur both allowed and induced moments must have the same symmetry. The allowed moment is described by the coefficient $A_1(100)$ and from (5) it may be deduced that the isotropic and anisotropic overlap induced moments contain a component of that symmetry.[3,20] This component is always parallel or antiparallel to the allowed moment, producing, respectively, constructive or destructive interference[19,21] (Fig. 2). In the HD-HD system, the matrix elements of the isotropic overlap induced moment vanish for 0-0 transitions.

Within the impact approximation, the line shape is again Lorentzian. This feature is sharp because the correlation function restricts possible transitions to those diagonal in translational states.[19] Experimental results of McKellar[1] for the fundamental and overtone bands showed asymmetric line shapes of the Fano type. Herman et al.,[5,21] to account for these, introduced into the correlation function dipole-weighted phase factors which represent the influence of phase shifts occurring at the end points of the time interval of the dipole-producing collisions. The correlation function is multiplied then by the complex quantity $\Delta = \Delta' + i\Delta''$ and the line shape is the sum of a Lorentzian and a dispersion contour. If the phase shifts during collision are large, both Δ' and Δ'' approach zero and the interference feature vanishes despite the fixed phase relationship of the allowed and induced moments. For the hydrogens, Δ' is apparently sizeable and a strong interference feature is possible.

3. Induced-induced

The contribution $\langle \mu_{12}^I(0)\cdot\mu_{13}^I(t)\rangle$ to the total correlation function involves three molecules and the absorption coefficient depends on ρ^3. The collision is still binary as the three molecules do not collide simultaneously.[4,21,22] This intercollisional interference contribution for HD involves the $A_1(100)$ component of the induced moment and is scalar in R. For uncorrelated collisions, the average value of $\langle J \,|\, p^I(R) \,|\, J'\rangle$ in a collision
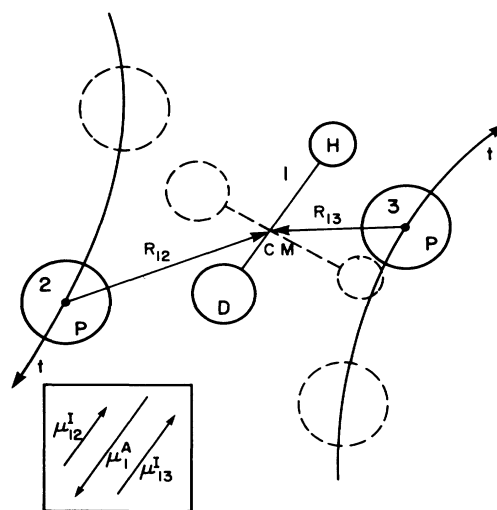

FIG. 2. Symbolic representation of the interaction of an HD molecule with two perturbers at two successive points in time. The induced moment component μ^I which contributes to the interference is always parallel or antiparallel to the allowed dipole moment. For the μ_{12}^I shown, the allowed-induced interference is destructive (antiparallel moments).

of a given molecule is independent of the value resulting from a subsequent collision. The translational correlation function is then always positive and

$$\langle \mu_{12}^I(0)\cdot\mu_{13}^I(t)\rangle = \{\langle J \,|\, p^I(R) \,|\, J'\rangle\}^2 \,,$$

where $\{\ldots\}$ denotes an ensemble average. Thus there always exists a positive intercollisional interference, which is referred to as scalar as opposed to the vector intercollisional interference in the homonuclear hydrogens.[4] The spectral features are characterized by the same parameters as are the allowed lines and, as in the case of the allowed-induced interference, the line shape is the sum of a Lorentzian and dispersion profile.

4. The total spectrum

The total absorption coefficient from the allowed, allowed-induced, and induced-induced contributions is[5]

$$\alpha(\omega) = \rho N_0 (4\pi^2/3\hbar c)\omega(J+1)P(J)\,|\,\langle J\,|\,p^A(r)\,|\,J'\rangle\,|^2$$

$$\times \left[[1 + 2\rho N_0\Delta'I + \rho^2 N_0^2(\Delta'^2 - \Delta''^2)I^2]\frac{(\gamma/2\pi)}{(\gamma/2)^2 + (\omega-\omega_0)^2} + (\rho N_0\Delta''I + \rho^2 N_0^2\Delta'\Delta''I^2)\frac{2(\omega-\omega_0)/\pi}{(\gamma/2)^2 + (\omega-\omega_0)^2} \right]$$

$$\tag{6}$$

with

$$I = 4\pi\frac{\int_0^\infty \langle J\,|\,p^I(R)\,|\,J'\rangle g(R)R^2 dR}{\langle J\,|\,p^A\,|\,J'\rangle} \,. \tag{7}$$

The shifted peak is at ω_0, γ is the full width at half maximum (FWHM), $P(J)$ is the normalized Boltzmann factor for the initial state with rotational quantum number J, and $g(R)$ is the pair distribution function. The integrated intensity is

$$\int_{-\infty}^{\infty} [\alpha(\omega)/\rho N_0\omega]d\omega = \int_{-\infty}^{\infty} [\alpha^A(\omega)/\rho N_0\omega]d\omega[1+2\rho N_0\Delta'+\rho^2 N_0^2(\Delta'^2-\Delta''^2)I^2] \; , \tag{8}$$

where $\alpha^A(\omega)$ is the absorption coefficient associated with the allowed moment alone. The phase shifts Δ' and Δ'' depend on the species and temperature and have not been evaluated. If the time of duration of collisions is taken into account, further intensity and asymmetry effects are introduced[12] (see paper II).

HD is the simplest example of the so-called "loaded sphere." The intermolecular potential is nearly symmetric about a center of force, but it has a large effective anisotropy due to an eccentric rotation about an axis displaced by $r_e/6$ towards the deuterium end of the molecule. If this anisotropic part of the potential is included in the analysis, then mixing of translational and rotational states may occur. Tabisz and Nelson[23] have developed an approach to estimate the effect of this mixing on the interference terms. In their treatment, the mixing makes measurable contributions to the allowed-induced absorption coefficient.

III. EXPERIMENTAL DETAILS

The technique used was essentially that of our earlier studies[7,8] but significant improvements were made both in apparatus and procedures. The dried sample gases were contained in a 1-m stainless-steel absorption cell equipped with polythylene windows. Absorption spectra were recorded in the range 80–375 cm^{-1} with a Nicolet FTIR (Fourier transform infrared) interferometer modified to accept a long-path-length sample cell. All experiments were performed at 295 K at about 40 different densities in the range 2–68 amagat. The light source was a globar and the detector was a helium-cooled composite germanium bolometer. A 375-cm^{-1} far-infrared cut-on type filter, consisting of wedged sapphire, diamond, and ZnO, was located in the entrance to its cavity in order to reject unwanted incident radiation. The interferometer was operated at its maximum resolution, nominally 0.06 cm^{-1}. The installation of the bolometer greatly improved the signal-to-noise ratio over our previous studies[7,8] and was responsible for the acquisition of much superior data.

The presence of water vapor along the optical path was a major concern. Some parts of the apparatus could be evacuated, others were purged with gas produced by boiling liquid nitrogen. A small amount of water vapor nevertheless was always present ($\sim$0.5 mg/l). Fortunately, in the process of taking the ratio of the intensities transmitted by the evacuated and the filled cell to obtain the absorption coefficient, the lines due to water were effectively removed from the spectrum.

The gas samples (supplied by Merck, Sharp, and Dhome) were independently mass spectrometrically analyzed to obtain the precise amounts of HD, D_2, and H_2 present. The HD concentration was usually about 98%. The sample bottles were immersed in liquid nitrogen to condense water vapor present before the gas was allowed to expand slowly into the cell. Gas pressures were con-

verted to amagat densities with an equation of state incorporating the second virial coefficient.[24]

Water lines served as an internal frequency calibration with the highly accurate frequency tabulation of Johns[25] taken as the primary standard. A linear relation sufficed to describe deviations between measured and true frequencies.

The collected interferograms were processed using the fast Fourier transform algorithm and Happ-Genzel apodization. In some spectra, an oscillation, caused by multiple reflections from the parallel surfaces of the cell windows, modulated the absorption profiles. Although it is possible to eliminate this noise by removing the corresponding signatures in the interferogram, it was decided not to do so since such a procedure might result in modification of the line intensities. This type of noise has no effect on the integrated absorption.

The four rotational lines of interest, $R(0)$–$R(3)$, appeared as sharp features superimposed on a collision-induced background due to the translational spectrum and the induced $S_0(0)$ and $S_0(1)$ lines. An example of an absorbance $\{\log_{10}[I_0(\omega)/I(\omega)]\}$ spectrum is given in Fig. 3. Because the S_0 lines are broad ($\sim$100 cm^{-1}), they simply provided a continuous baseline and were removed by fitting a quadratic expression in a 10-cm^{-1} in-
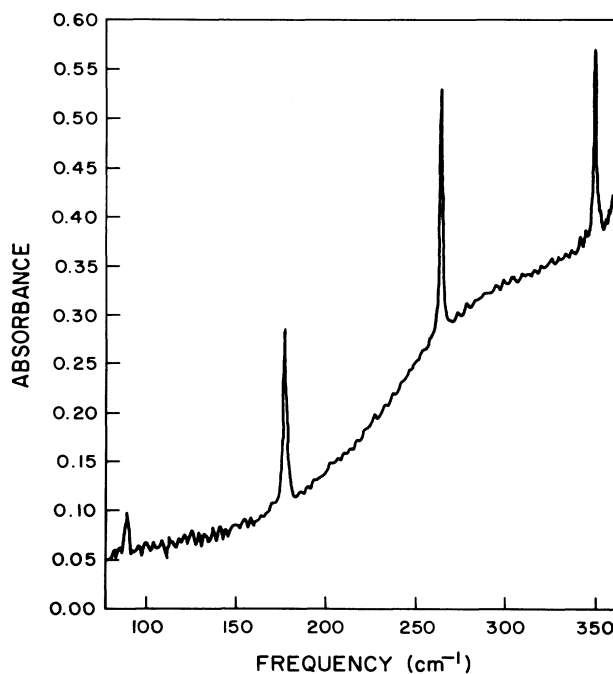

FIG. 3. The far-infrared absorbance spectrum $[\log_{10}I_0(\omega)/I(\omega)]$ of pure HD at 68 amagat and 1 cm^{-1} resolution. The sharp features at 89 cm^{-1}, 178 cm^{-1}, 265 cm^{-1}, and 351 cm^{-1} are the allowed rotational lines $R(0)$ to $R(3)$. They sit on the broad collision-induced background.

terval about each rotational line. Since the water lines had been effectively eliminated in the procedure of taking the intensity ratio, no further connection was necessary for them.

IV. ANALYSIS OF DATA

Each rotational line was fitted with a theoretical line shape and the integrated intensity, width, and peak frequency determined as functions of density. The lineshape function employed[1,3] was alternative, but equivalent, to (6),

$$\alpha(\omega)/\rho N_0\omega = (D_0\gamma\pi/2)\left[(1-q^{-2})\frac{(\gamma/2\pi)}{(\gamma/2)^2+(\omega-\omega_0)^2}\right.$$
$$\left.+q^{-1}\frac{2(\omega-\omega_0)/\pi}{(\gamma/2)^2+(\omega-\omega_0)^2}\right] . (9)$$

It is thus the sum of Lorentzian and dispersion contribu-

tions. The dimensionless parameter q describes the line asymmetry. When $q^{-1}=0$, the line is Lorentzian and q is related to Δ by[3]

$$q^{-1}=\rho N_0\Delta''I/(1+\rho N_0\Delta'I) . (10)$$

It must be emphasized that (9) is a general expression for a Fano-type profile and is independent of the theory of Herman et al.;[3] the connection to the theory occurs through (10).

A constant term was added to (9) to improve further on the baseline connection described in Sec. III. Both the Marquardt and Gauss-Newton algorithms for nonlinear fitting gave identical results for the five free parameters. Careful observation of the experimental spectra reveals an occasional small asymmetry. For most cases, the fitting procedure gave large positive values to q which correspond to a pure Lorentzian profile. Figures 4 and 5 show the observed $R(1)$ and $R(2)$ lines at four densities together with the fitted profiles.
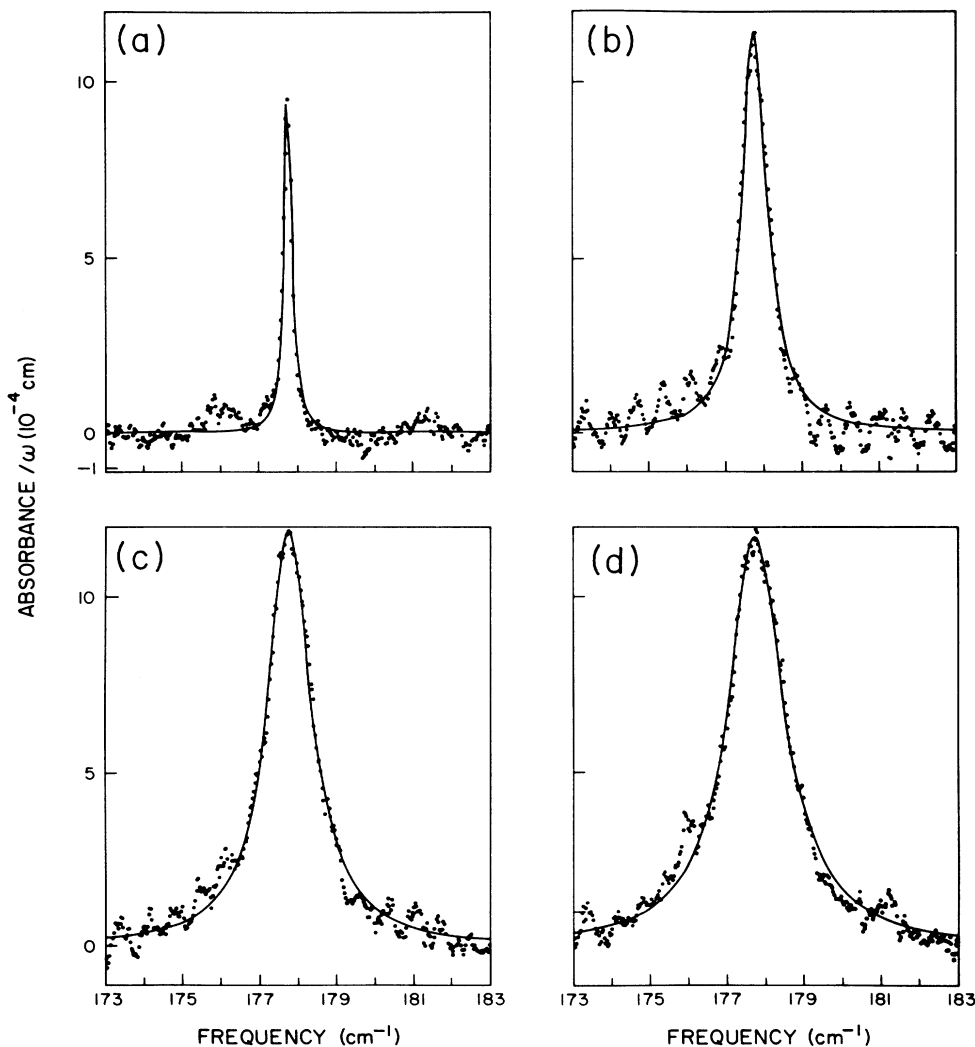

FIG. 4. Ratio of absorbance to frequency for the $R(1)$ line of pure HD at (a) 6.9 amagat, (b) 28.4 amagat, (c) 51.8 amagat, (d) 63.4 amagat. Points are experimental. Solid line is the fitted profile [Eq. (9)]. Resolution: 0.06 cm^{-1}.

The integrated absorption was calculated analytically,

$$\int [\alpha(\omega)/\rho N_0 \omega] d\omega = D_0 \gamma (1 - q^{-2}) \arctan(2z) , \quad (11)$$

where z is the number of widths about ω_0 for which the integration is extended; here six widths served as the range of integration. The integrated absorption coefficient can be expanded in powers of the density,

$$\int [\alpha(\omega)/\rho_a N_0 \omega] d\omega = c_0 + c_1 \rho + c_2 \rho^2 . \quad (12)$$

The density ρ_a is that of the "absorber" and ρ is that of the "perturber." For the case of a pure HD sample, ρ_a and ρ both refer to the density of HD.

From (8) and (12), it may be seen that

$$c_0 = (4\pi^2 N_0/3\hbar c)(J + 1)P(J) | \langle J | p^A(r) | J' \rangle |^2 , \quad (13)$$

$$c_1 = c_0(2N_0 \Delta' I) , \quad (14)$$

$$c_2 = c_0 N_0^2(\Delta'^2 - \Delta''^2)I^2 . \quad (15)$$

To account for stimulated emission, $P(J)$ is written as

$$P(J) = \frac{\exp(-E_i/kT) - \exp(-E_f/kT)}{\sum_j (2J + 1)\exp(-E_j/kT)} ,$$

where i and f refer to the initial and final states.

The fitting of (12) to the data was attempted through three different approaches: (a) assuming $c_2 = 0$, which means that the intercollisional interference effect is negligible, (b) ignoring constraint (10) which then allows the free fitting of a quadratic polynomial, and (c) using (10), (13), (14), and (15) to fit an expression conforming fully to the existing theory. In all cases, the data were weighted with the variances of the integrated absorption coefficients which were obtained by combining the variances of the line parameters. Only method (c) consistently gave results which realistically described the data. Figure 6 shows the fitted curve for $R(3)$.

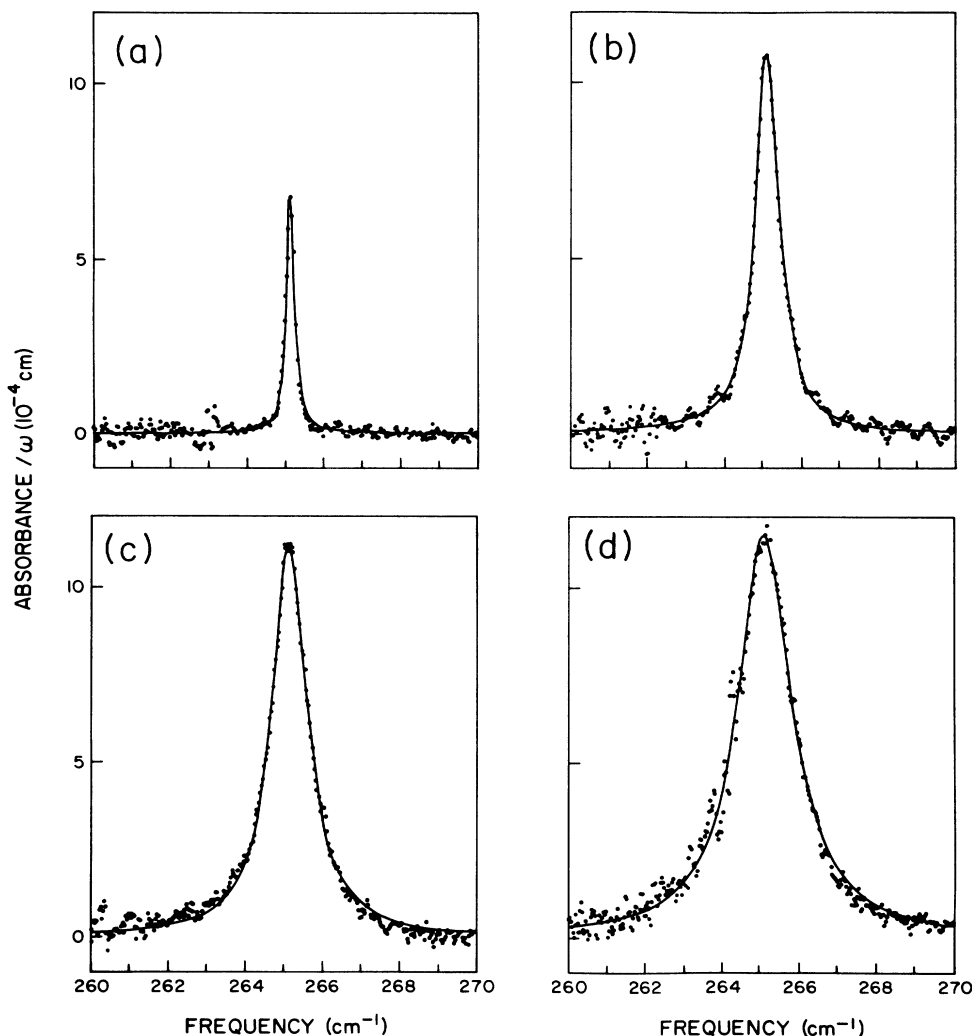The magnitude of the permanent dipole moment can be obtained from (13) as

FIG. 5. Ratio of absorbance to frequency for the $R(2)$ line of pure HD at (a) 6.9 amagat, (b) 31.4 amagat, (c) 46.5 amagat, (d) 68.3 amagat. Points are experimental. Solid line is the fitted profile [Eq. (9)]. Resolution: 0.06 cm^{-1}.
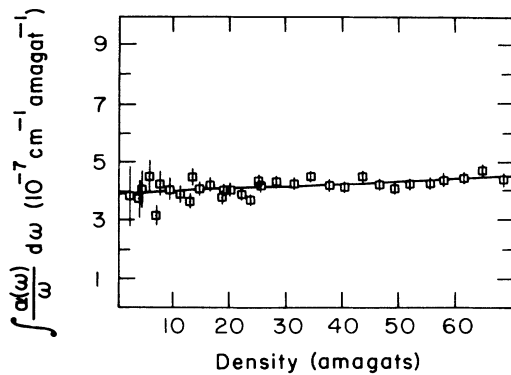
FIG. 6. Integrated absorption coefficient of $R(3)$ of pure HD as a function of density. Points are experimental. Solid line is the fitted curve [Eq. (12), method (c)].

$[c_0/(4\pi^2 N_0/3\hbar c)(J+1)P(J)]^{1/2}$ and these values are given in Table I. It is convenient to introduce two other parameters $a = c_1/c_0$ and $b = c_2/c_0$. Clearly a denotes the relative magnitude of the allowed-induced interference and b the relative magnitude of the intercollisional interference. The values of a are presented in Table I. These values are not affected by the choice of the limit of integration z.

The linewidth γ (FWHM) of $R(1)$ is plotted function of density in Fig. 7. According to pressure broadening theory, in the impact approximation γ should depend linearly on density,

$$\gamma = B_0\rho + K_1 . \tag{16}$$

The values of B_0 determined are listed in Table I. The location of the line peak as a function of density could also be described by a linear relation

$$\omega_0 = S_0\rho + \omega_0^0 . \tag{17}$$

The shift parameters S_0 and the zero-density frequencies ω_0^0 are presented in Table I. The uncertainties given for the tabulated quantities are the 1σ values deduced in the fitting procedure.

This is a good point to assess the quality of the measured data and of the analysis. Again, the observed lines were found to be generally symmetrical. The asymmetry parameter q^{-1} was practically zero and the fitted line shape was Lorentzian. This fact has minimal effect on the intensities and widths but does have implication for the line position, since a frequency shift other than that predicted in the pressure broadening theory is introduced through the dispersion curve incorporated within the Fano-type line shape. The discussion of collisional interference effects will be concerned only with the parameter a; because of the symmetric lineshape, $\Delta''=0$ and b reduces to $(a/2)^2$ and is thus always related to the value of a.

The number of absorbers and the signal-to-noise ratio increase with density. The large number of densities at which data were taken enhances the statistical significance of the parameters derived from the fitted

curves. The errors quoted in Table I represent the statistical error in the fitting procedure. There is the possibility of systematic error; for example, $R(1)$ is superimposed upon a water line and despite the great reduction of water vapor in the sample achieved by cooling the gas bottle, some vapor might remain. In the region of $R(3)$ and particularly $R(0)$, the interferometer system has a poor intensity response and statistical uncertainties arise in the recorded data. There is then variation in the quality of the data from line to line. $R(2)$ can be considered best, followed by $R(1)$, $R(3)$, and $R(0)$.

A. Discussion of results

In this section the results are critically assessed and compared with previously reported experiments.

1. Dipole moment

In Table I, other experimental and theoretical values of the permanent dipole of HD are also listed. Those of Trefler and Gush[6] are clearly low. The results of Nelson and Tabisz[8] follow the same pattern with J as do those of the present study but show an overall trend to a larger magnitude. There is excellent agreement for $R(3)$ with Essenwanger and Gush.[10] The values of McKellar[11] are perhaps slightly lower.

The average difference between the present results and the *ab initio* calculations is 4% but there is a J dependence larger than predicted by the theory. The large number of densities at which spectra were collected reduces the statistical error in the present work. Since the J dependence remains outside statistical and estimated systematic error, it is taken to be real. However, for $R(0)$ and $R(1)$ when the measured integrated absorption coefficient is plotted against density, there is a slight downward curvature of the integrated absorption results at very low densities (less than 10 amagat). If this curvature is real, the actual dipole moment would be lower than that reported and there would be a smooth increase of dipole moment with J.

2. Allowed-induced interference

In Table I, the parameter a is compared with earlier results. There is very good agreement with the results of McKellar except for $R(2)$, but there is a discrepancy with the values of Essenwanger and Gush[10] and of Nelson and Tabisz.[8] The large interference parameters reported in the latter study arose from the manual fitting of the line shape function to low-resolution spectral data. The high values of a thus found also explain, because of the extrapolation of the integrated absorption coefficient data to zero density, the high values of the dipole moment reported in Ref. 8.

3. Profile parameters

The broadening coefficients agree well with previous work, except for the $R(3)$ value of McKellar[11] (Table I). Although the interferometer used for the present experiments does not permit highly accurate frequency deter-

minations, the unshifted line positions are generally consistent with other reports (Table I). The frequency shift coefficients are small and 75% lower than those of McKellar.[11] This result occurs because of the different line-shape functions found appropriate in the two studies. McKellar found that a Fano profile could be fitted to his asymmetric profiles. In the present work, the almost Lorentzian contour returned by the fitting procedure does not produce a peak shift from the line center in the same manner as does the Fano function with its density dependent dispersion component.

V. COMPARISON WITH THEORY OF INTERFERENCE

The numerical computation of the interference effects following existing theories poses some problems. Even if the theory adequately describes the data, quantities that enter the calculation, such as the strength of the allowed and induced moments and the pair distribution function, must be known accurately. The quantities a and b can be estimated [Eqs. (14) and (15)]. The phase shift Δ, even in its simplest form, is difficult to evaluate.[5] In the

TABLE I. Spectral properties of HD from experiment and theory. Uncertainty in the last quoted figure(s) appears in parentheses.

	$R(0)$	$R(1)$	$R(2)$	$R(3)$
	Dipole moment p^A (10^{-4} D)			
	Experiment			
Present work	8.83(28)	7.94(2)	7.88(3)	8.43(10)
Trefler[a]	5.42	5.52	6.18	6.41
Nelson[b]		8.78(20)	8.47(20)	10.21(20)
Essenwanger[c]				8.47(9)
McKellar[d]		7.5(4)	7.8(4)	7.4(4)
McKellar[e]	8.18(26)	7.9(4)		
	Theory			
Wolniewicz[f]	−8.36	−8.38	−8.39	−8.41
Ford and Browne[g]	−8.31	−8.30	−8.28	−8.26
Thorson et al.[h]	−8.463	−8.455	−8.440	−8.420
Bishop and Cheung[i]	−8.65			
	Interference parameter a (10^{-3} amagat^{-1})			
	Experiment			
Present work	−2.5(19)	−1.1(2)	+1.3(1)	+2.1(6)
Nelson[b]		−7.7(12)	−6.3(12)	−7.2(11)
Essenwanger[c]				−260(70)
McKellar[d]		−1.5(3)	−2.0(3)	+2.4(3)
	Calculation			
a	2.3	2.3	2.3	2.3
Δa	0.8	0.9	0.3	0.9
$a + \Delta a$	3.1	3.2	2.6	3.2
	Broadening coefficient B_0 (10^{-2} cm^{-1} amagat^{-1})			
Present work	3.32(16)	2.53(1)	2.20(1)	1.81(3)
Essenwanger[c]				1.83(1)
McKellar[d]		2.44(2)	2.26(2)	1.99(2)
	Line frequency ω_0^0 (cm^{-1})			
Present work	89.19(1)	177.84(1)	265.23(1)	350.85(1)
Essenwanger[c]				350.852(2)
McKellar[d]		177.828(2)	265.207(2)	350.844(2)
	Frequency shift coefficient S_0 (10^{-3} cm^{-1} amagat^{-1})			
Present work	+3.5(5)	+0.6(1)	+0.6(1)	−0.4(1)
McKellar[d]		+2.4(2)	+2.9(2)	+1.3(1)

[a]Reference 6.
[b]Reference 8.
[c]Reference 10.
[d]Reference 11.
[e]Reference 9.
[f]Reference 15.
[g]Reference 16.
[h]Reference 17.
[i]D. Bishop and L. M. Cheung, Chem. Phys. Lett. **55**, 598 (1978).

"gentle encounter" limit, Δ remains real; therefore $\Delta'=1$ and $\Delta''=0$ and the interference parameter a appears in a computable form,

$$a=2N_0I \ ,$$

$$b=N_0^2I^2=a^2/4 \ . \tag{18}$$

The induced dipole component in I originates from overlap coefficients. The analytical form of A_{Λ} for H_2-H_2 has been determined in *ab initio* fashion by Meyer.[26] In general,

$$A_{\Lambda}(\lambda_1,\lambda_2,\lambda;R)=(A^{(7)}/R^7)$$
$$+A^{(0)}\exp[b_1(R-\sigma)+b_2(R-\sigma)^2] \ , \tag{19}$$

where σ is the molecular diameter. The first term accounts for a small long-range dispersion contribution
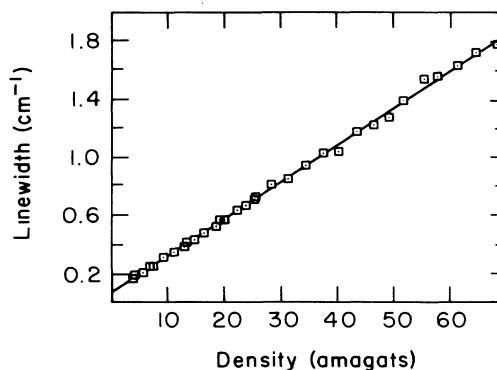

FIG. 7. Broadening coefficient of the $R(1)$ line of pure HD as a function of density. Points are experimental. Solid line is the fitted curve [Eq. (16)].

and the second for the exchange and distortion effects.

The functions $A_0(001)$ and $A_2(201)$ can be shifted by (5) to obtain the $A_1(100)$ components for HD (labeled $[A_1(100)]_0$ and $[A_1(100)]_2$, respectively). If

$$Z(R)=(r_1/18)\{-5A^{(7)}/R^8+[(2/R)+b_1+2b_2(R-\sigma)]A^{(0)}\exp[b_1(R-\sigma)+b_2(R-\sigma)^2]\} \ , \tag{20}$$

then

$$[A_1(100)]_0=Z(R) \text{ from } A_0(001) \ ,$$

and

$$[A_1(100)]_2=-\sqrt{2}Z(R) \text{ from } A_2(201) \ . \tag{21}$$

For HD-HD, there is no contribution from $A_0(001)$ since it has essentially zero matrix elements for the pure rotational transitions.[27] The J dependence of the matrix elements of $p^I(R)$ is negligible[3] and

$$\langle J \mid p^I(R) \mid J' \rangle=[A_1(100)]_2 \ .$$

The required parameters were estimated by fitting an exponential function to the numerical data of Meyer for $A_2(201)$ in the region of $R=\sigma(3.019 \text{ Å})$. These were found to be $A^{(7)}=0$, $A^{(0)}=1.659\times10^{-3}$ D, $b_1=-3.180$ Å^{-1}, and $b_2=0$.

The zeroth-order approximation to the classical distribution function was taken; $g(R)=\exp[-V(R)/kT]$, where $V(R)$ is the intermolecular potential function. The HFD (Hartree-Fock-dispersion)-type potential of Norman *et al.*[28] for H_2-H_2 was adopted. It was transformed to the HD system by[29]

$$V(\text{HD})=V(H_2)-(r_e/6)(dV/dR)\cos\gamma \ , \tag{22}$$

where γ is the angle between the intermolecular and internuclear axis. Then

$$\langle J \mid p^I(R) \mid J' \rangle=\int \int \int p^I(R)\exp\{-[V(R)-(r_e/6)(dV/dR)\cos\gamma]/kT\}R^2\sin\gamma \ dR \ d\gamma \ d\phi \ .$$

Expansion of the small exponential cosine term and integration over γ and ϕ yields for (7)

$$I=\frac{4\pi}{\langle J \mid p^4 \mid J' \rangle} \int_0^{\infty} p^I(R)\{\exp[-V(R)/kT]+(r_e^2/216kT)(dV/dR)^2\}R^2dR \ , \tag{23}$$

which can be evaluated numerically. The interference parameter a was calculated from (18) and (23) and found to be 2.3×10^{-3} amagat^{-1}.

In addition, calculation of the effect Δa of rotational level mixing by the anisotropy of the potential can be estimated according to the prescription of Ref. 23. From Table I, it is seen that there is good agreement between the magnitude of the calculated interference parameter a and the measured value. The estimated Δa may be too large. In paper II, an argument is presented that allows, in some cases, prediction of the sign of a. Further comment on the comparison between experiment and theory is made there where the results for a number of different perturber gases are presented.

VI. SUMMARY

The permanent dipole moment of HD has been found for the first four rotational transitions $R(0)$ to $R(3)$. The values are in good agreement with calculation except for some rotational state dependence. The collisional interference parameter is negative for $R(0)$ and $R(1)$ and positive for $R(2)$ and $R(3)$. The line shapes were found to be largely symmetrical and Lorentzian. Line-shape parameters agreed with the results of earlier studies.

[1]A. R. W. McKellar, Can. J. Phys. **51**, 389 (1973).

[2]J. D. Poll, R. H. Tipping, R. D. G. Prasad, and S. P. Reddy, Phys. Rev. Lett. **36**, 248 (1976).

[3]R. H. Tipping, J. D. Poll, and A. R. W. McKellar, Can. J. Phys. **56**, 75 (1978).

[4]R. M. Herman, Phys. Rev. Lett. **42**, 1206 (1979).

[5]R. M. Herman, R. H. Tipping, and J. D. Poll, Phys. Rev. A **20**, 2006 (1979).

[6]M. Trefler and H. P. Gush, Phys. Rev. Lett. **20**, 703 (1968).

[7]J. B. Nelson and G. C. Tabisz, Phys. Rev. Lett. **48**, 1393 (1982); **48**, 1870(E) (1982).

[8]J. B. Nelson and G. C. Tabisz, Phys. Rev. A **28**, 2157 (1983).

[9]A. R. W. McKellar, J. W. C. Johns, W. Majewski, and N. H. Rich, Can. J. Phys. **62**, 1673 (1984).

[10]P. Essenwanger and H. P. Gush, Can. J. Phys. **62**, 1680 (1984).

[11]A. R. W. McKellar, Can. J. Phys. **64**, 227 (1986).

[12]P. G. Drakopoulos and G. C. Tabisz, Phys. Rev. A **36**, 5566 (1987).

[13]See, for example, *Phenomena Induced by Intermolecular Interactions,* edited by G. B. Birnbaum (Plenum, New York, 1985).

[14]G. C. Wick, Atti R. Accad. Naz. Lincei, Mem. Cl. Sci. Fis. Mat. Nat. **21**, 708 (1935).

[15]L. Wolniewicz, Can. J. Phys. **54**, 672 (1976).

[16]A. L. Ford and J. C. Browne, Phys. Rev. A **16**, 1992 (1977).

[17]W. R. Thorson, J. H. Choi, and S. K. Knudson, Phys. Rev. A **31**, 22 (1985); **31**, 34 (1985).

[18]J. D. Poll and J. Van Kranendonk, Can. J. Phys. **39**, 189 (1961).

[19]J. D. Poll, in *Phenomena Induced by Intermolecular Interactions,* edited by G. B. Birnbaum (Plenum, New York, 1985), p. 677.

[20]R. H. Tipping and J. D. Poll, in *Molecular Spectroscopy: Modern Research,* edited by K. N. Rao (Academic, New York, 1985), Vol. III, p. 421.

[21]R. M. Herman, in *Proceedings of the 8th International Conference on Spectral Line Shapes,* edited by R. Exton (Deepak, Hampton, 1987).

[22]J. Van Kranendonk, Can. J. Phys. **46**, 1173 (1968).

[23]G. C. Tabisz and J. B. Nelson, Phys. Rev. A **31**, 1160 (1985).

[24]J. H. Dymond and E. B. Smith, *The Virial Coefficients of Pure Gases and Mixtures* (Clarendon, Oxford, 1980).

[25]J. W. C. Johns, J. Opt. Soc. Am. **B2**, 1340 (1985).

[26]W. Meyer, in *Phenomena Induced by Intermolecular Interactions,* edited by G. Birnbaum (Plenum, New York, 1985), p. 29.

[27]J. D. Poll and J. L. Hunt, Can. J. Phys. **54**, 461 (1976).

[28]M. J. Norman, R. O. Watts, and U. Buck, J. Chem. Phys. **81**, 3500 (1984).

[29]H. Kreek and R. J. LeRoy, J. Chem. Phys. **63**, 338 (1975).